Fiber Bragg Grating Technology Fundamentals and Overview

Kenneth O. Hill and Gerald Meltz, *Member, IEEE*

(Invited Paper)

***Abstract*— The historical beginnings of photosensitivity and fiber Bragg grating (FBG) technology are recounted. The basic techniques for fiber grating fabrication, their characteristics, and the fundamental properties of fiber gratings are described. The many applications of fiber grating technology are tabulated, and some selected applications are briefly described.**

***Index Terms*—Bragg gratings, optical fiber devices, optical fiber dispersion, optical fiber filters, optical fiber sensors, optical planar waveguides and components, photosensitivity.**

I. Introduction

A FIBER Bragg grating (FBG) is a periodic perturbation of the refractive index along the fiber length which is formed by exposure of the core to an intense optical interference pattern. The formation of permanent gratings in an optical fiber was first demonstrated by Hill *et al.* in 1978 at the Canadian Communications Research Centre (CRC), Ottawa, Ont., Canada, [1], [2]. They launched intense Argon-ion laser radiation into a germania-doped fiber and observed that after several minutes an increase in the reflected light intensity occurred which grew until almost all the light was reflected from the fiber. Spectral measurements, done indirectly by strain and temperature tuning of the fiber grating, confirmed that a very narrowband Bragg grating filter had been formed over the entire 1-m length of fiber. This achievement, subsequently called "*Hill gratings*," was an outgrowth of research on the nonlinear properties of germania-doped silica fiber. It established an unknown photosensitivity of germania fiber, which prompted other inquires, several years later, into the cause of the fiber photo-induced refractivity and its dependence on the wavelength of the light which was used to the form the gratings. Detailed studies [3] showed that the grating strength increased as the square of the light intensity, suggesting a two-photon process as the mechanism. In the original experiments, laser radiation at 488 nm was reflected from the fiber end producing a standing wave pattern that formed the grating. A single photon at one-half this wavelength, namely at 244 nm in the ultraviolet, proved to be far more effective. Meltz *et al.* [4] showed that this radiation could be used to form gratings that would reflect any wavelength by illuminating the fiber through the side of the cladding with two intersecting beams of UV light; now, the period of the interference maxima and the index change was set by the angle between the beams and the UV wavelength rather than by the visible radiation which was launched into the fiber core. Moreover, the grating formation was found to be orders-of-magnitude more efficient.

At first, the observation of photo-induced refractivity in fibers was only a scientific curiosity, but over time it has become the basis for a technology that now has a broad and important role in optical communications and sensor systems. Research into the underlying mechanisms of fiber photosensitivity and its uses is on-going in many universities and industrial laboratories in Europe, North and South America, Asia, and Australia. Several hundred photosensitivity and fiber grating related articles have appeared in the scientific literature and in the proceedings of topical conferences, workshops, and symposia. FBG's are now commercially available and they have found key applications in routing, filtering, control, and amplification of optical signals in the next generation of high-capacity WDM telecommunication networks.

This article contains an introduction to the fundamentals of FBG's, including a description of techniques for grating fabrication and a discussion of those fiber photosensitivity characteristics which underlie grating formation. We highlight the salient properties of periodic, optical waveguide structures that are used in the design of grating filters and conclude with an overview of key applications in optical telecommunications and quasidistributed, thermophysical measurement. Other articles and reviews of the technology that have appeared include a recent comprehensive article by Bennion *et al.* [5] and survey papers that discuss the physical mechanisms that are believed to be important in photosensitivity [6] and applications of gratings to fiber optic sensors [7].

II. Photosensitivity and Grating Formation

Fiber photosensitivity was first observed in the experimental arrangement showed in Fig. 1. Continuous wave blue (488 nm) light from an Argon ion laser is launched into a short piece of nominally monomode optical fiber and the intensity of the light reflected back from the fiber is monitored. Initially, the reflected light intensity is low, but after a period of few minutes, it grows in strength until almost all the light launched into the fiber is back-reflected. The growth in back-reflected light was explained in terms of a new nonlinear effect called "*photosensitivity*" which enables an index grating to be

Manuscript received May 13, 1997; revised May 19, 1997.

K. O. Hill is with the Communications Research Center, Ottawa, Ont. K2H 8S2 Canada.

G. Meltz is with OFT Associates, Avon, CT 06001 USA.

Publisher Item Identifier S 0733-8724(97)05932-X.

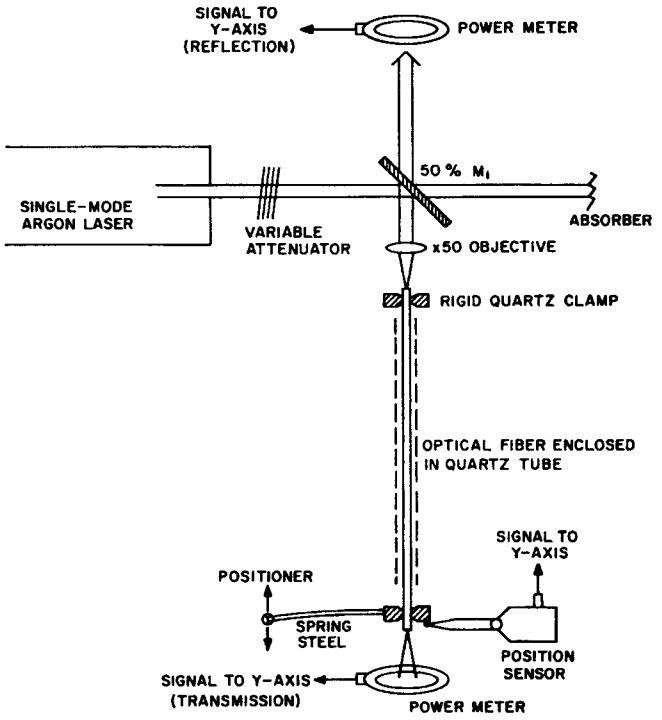

Fig. 1. Schematic of original apparatus used for recording Bragg gratings in optical fibers. A position sensor monitored the amount of stretching of the Bragg grating as it was strain-tuned to measure its very narrow-band response.

written in the fiber. The reasoning is as follows. Coherent light propagating in the fiber interferes with a small amount of light reflected back from the end of the fiber to set up a standing wave pattern which through photosensitivity writes an index grating in the fiber core. As the strength of grating increases the intensity of the back-reflected light increases until it saturates near 100%. In these first experiments, permanent index gratings (Bragg gratings) with 90% reflectivity at the Argon laser writing wavelength were obtained. The bandwidth of the Bragg grating which was measured by stretching the fiber, is very narrow (<200 MHz) indicating a grating length of $\sim$1 m.

At the time, it was recognized that gratings in optical waveguides would have many potential applications in the fabrication of devices for use in fiber optic communications. In fact, it was shown that "*Hill gratings*" could be used as a feedback mirror for a laser and as a sensor for strain by stretching the fiber. Although photosensitivity appeared to be an ideal means for fabricating gratings in optical fibers, the "*Hill gratings*" unfortunately functioned only at light wavelengths in the visible close to the wavelength of the writing light. This limitation on photosensitivity was overcome about ten years later in an experiment by Meltz *et al.* [4] who recognized from the work of Lam and Garside [3] that photosensitivity was a two photon process that could be made much more efficient if it were a one photon process at a wavelength in the 5 eV (245 nm) germania oxygen-vacancy defect band [8], [9]. In their experiment, the fiber is irradiated from the side with two intersecting coherent ultraviolet light beams (see Fig. 2). The wavelength of the ultraviolet light is 244 nm which corresponds to one half of 488 nm, the wavelength of the blue Argon laser line used to produce the "*Hill gratings*." The two overlapping ultraviolet light beams interfere producing a periodic interference pattern that writes a corresponding periodic index grating in the core of the optical fiber. The technique called the transverse holographic technique is possible because the fiber cladding is transparent to the ultraviolet light whereas the fiber core is highly absorbing to the ultraviolet light.

The holographic technique for grating fabrication has two principal advantages. Bragg gratings could be photoimprinted in the fiber core without removing the glass cladding. Furthermore, the period of the photoinduced grating depends on the angle between the two interfering coherent ultraviolet light beams. Thus even though ultraviolet light is used to fabricate the grating, Bragg gratings could be made to function at much longer wavelengths in a spectral region of interest for devices which have applications in fiber optic communications and optical sensors.

III. Characteristics of Photosensitivity

When ultraviolet light radiates an optical fiber, the refractive index of the fiber is changed permanently; the effect is termed photosensitivity. The change in refractive index is permanent in the sense that it will last for decades (life times of 25 years are predicted) if the optical waveguide after exposure is annealed appropriately, that is by heating for a few hours at a temperature of 50 °C above its maximum operating temperature [10]. Initially, photosensitivity was thought to be a phenomenon associated only with germanium doped optical fibers. Subsequently, it has been observed in a wide variety of different fibers, many of which did not contain germanium as a dopant. Nevertheless, optical fiber having a germanium doped core remains the most important material for the fabrication of devices.

The magnitude of the refractive index change (Δn) obtained depends on several different factors such as the irradiation conditions (wavelength, intensity, and total dosage of irradiating light), the composition of glassy material forming the fiber core and any processing of the fiber prior to irradiation. A wide variety of different continuous wave and pulsed laser light sources with wavelengths ranging from the visible to the vacuum ultraviolet have been used to photo-induce refractive index changes in optical fibers. In practice, the most commonly used light sources are KrF and ArF excimer lasers that generate, respectively, 248 and 193 nm optical pulses (pulsewidth 10 ns) at pulse repetition rates of 50–75 pulses/s. The typical irradiation conditions are an exposure to the laser light for a few minutes at intensities ranging for 100–1000 mJ/cm^2. Under these conditions Δn is positive in germanium doped monomode fiber with a magnitude ranging between 10^{-5} to 10^{-3}. Techniques such as "hydrogen loading" [11] or "flame brushing" [12] are available which can used to process the fiber prior to irradiation in order to enhance the refractive index change obtained on irradiation. By the use of hydrogen loading a Δ as high as 10^{-2} has been obtained.

Irradiation at intensity levels higher than 1000 mJ/cm^2 mark the onset of a different nonlinear photosensitive process that

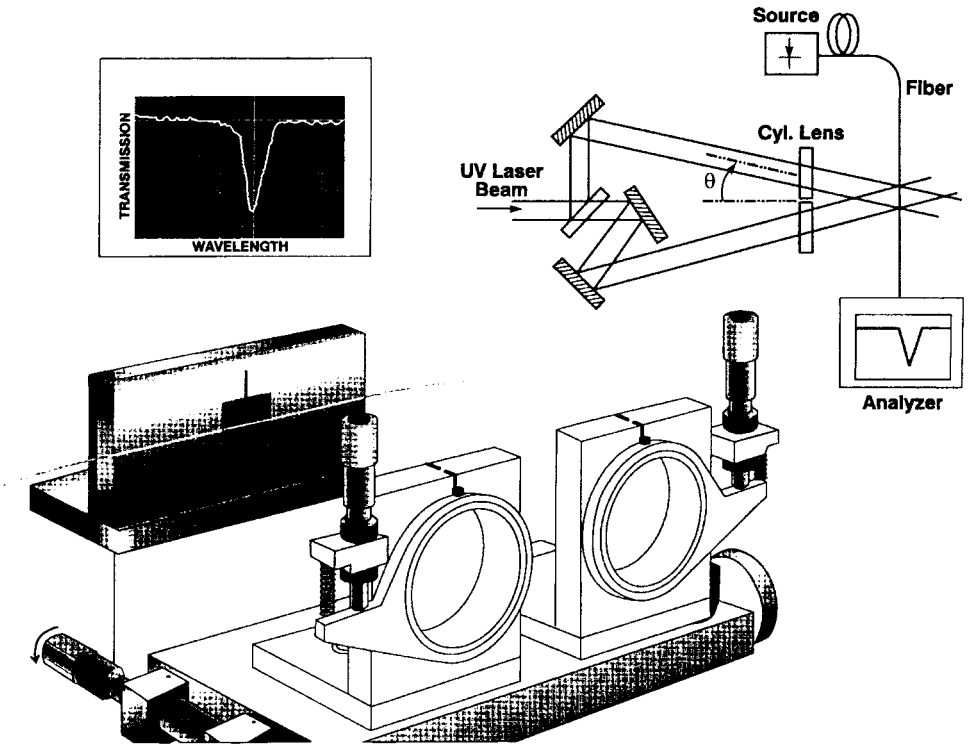

Fig. 2. Two-beam interferometer arrangement for side-writing fiber Bragg gratings (FBG's).

enables a single irradiating excimer light pulse to photoinduce a large index changes in a small localized region near the core/cladding boundary. In this case the refractive index changes are sufficiently large to be observable with a phase contrast microscope and have the appearance of damaging physically the fiber. This phenomenon has been used for the writing of gratings using a single excimer light pulse.

Another property of the photoinduced refractive index change is anisotropy. This characteristic is most easily observed by irradiating the fiber from the side with ultraviolet light polarized perpendicular to the fiber axis. The anisotropy in the photoinduced refractive index change results in the fiber becoming birefringence for light propagating through the fiber. The effect is useful for fabricating polarization mode converting devices or rocking filters [13].

The physical mechanisms underlying photosensitivity are not very well understood but are associated with the color centers in glassy materials. For example, UV photoexcitation of oxygen-vacancy-defect states [9] in Ge–SiO_2 fiber forms paramagnetic GeE′ centers that contribute to the index change [14]. There is also evidence that structural rearrangement of the glass matrix, possibly densification, is also correlated with the index increase [15]. The net result of the photoinduced changes is a permanent change in the refractive index of the glassy material at wavelengths far removed from the wavelength of the irradiating ultraviolet light.

IV. Grating Fabrication Techniques

Historically, Bragg gratings were first fabricated using the internal writing [1] and the holographic technique [4]. Both these methods, which have been described already, have been largely superseded by the phase mask technique [16], [17] which is illustrated in Fig. 3. The phase mask is made from flat slab of silica glass which is transparent to ultraviolet light. On one of the flat surfaces, a one dimensional periodic surface relief structure is etched using photolithographic techniques. The shape of the periodic pattern approximates a square wave in profile. The optical fiber is placed almost in contact with the corrugations of the phase as shown in Fig. 3. Ultraviolet light which is incident normal to the phase mask passes through and is diffracted by the periodic corrugations of the phase mask. Normally, most of the diffracted light is contained in the 0, $+1$, and -1 diffracted orders. However, the phase mask is designed to suppress the diffraction into the zero-order by controlling the depth of the corrugations in the phase mask. In practice the amount of light in the zero-order can be reduced to less than 5% with approximately 40% of the total light intensity divided equally in the ± 1 orders. The two ± 1 diffracted order beams interfere to produce a periodic pattern that photoimprints a corresponding grating in the optical fiber. If the period of the phase mask grating is Λ_{mask}, the period of the photoimprinted index grating is $\Lambda_{\mathrm{mask}}/2$. Note that this period is independent of the wavelength of ultraviolet light irradiating the phase mask; however, the corrugation depth required to obtain reduced zeroth-order light is a function of the wavelength and the optical dispersion of the silica.

The phase mask technique has the advantage of greatly simplifying the manufacturing process for Bragg gratings, yet yielding gratings with a high performance. In comparison with the holographic technique, the phase mask technique offers easier alignment of the fiber for photoimprinting, reduced stability requirements on the photoimprinting apparatus and lower coherence requirements on the ultraviolet laser beam

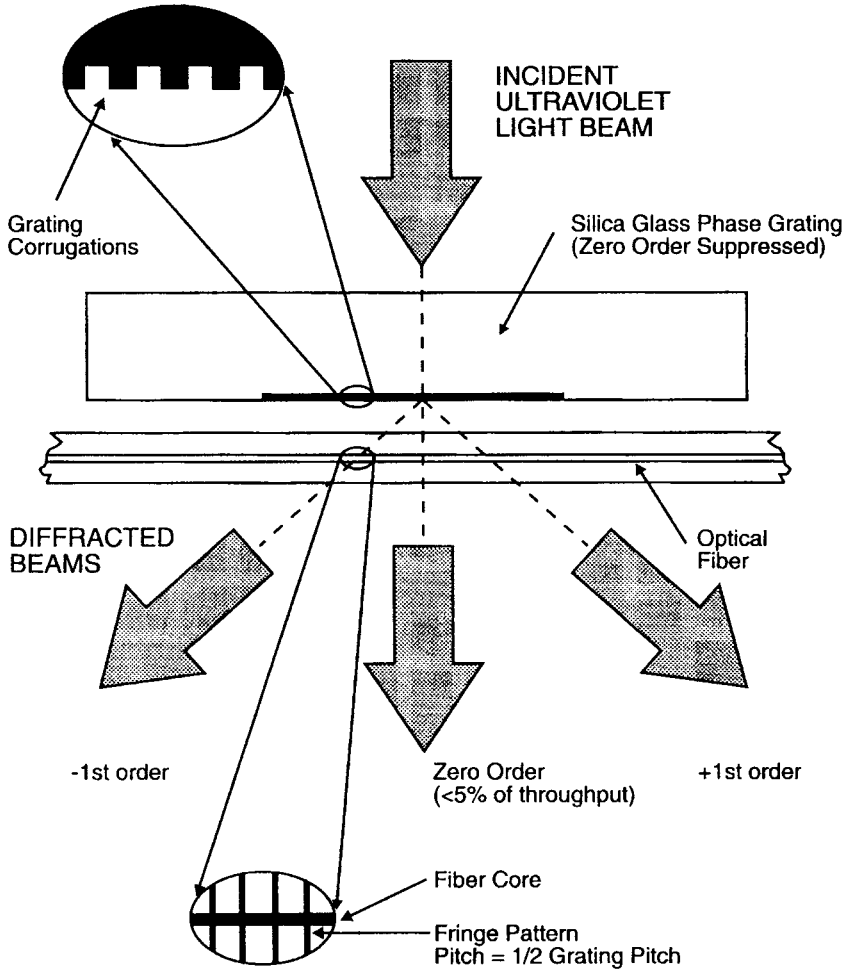

Fig. 3. Bragg grating fabrication apparatus based on a zero-order nulled diffraction phase mask. The duty cycle of the phase mask is chosen to be 50%. The amplitude of the phase mask groves is chosen to reduce the light transmitted in the zero-order beam to less than 5% of the total throughput. These choices result typically in more than 80% of the throughput being in the ± 1 diffracted beams.

thereby permitting the use a cheaper ultraviolet excimer laser source. Furthermore, there is the possibility of manufacturing several gratings at once in a single exposure by irradiating parallel fibers through the phase mask. The capability to manufacture high-performance gratings at a low per unit grating cost is critical for the economic viability of using gratings in some applications. A drawback of the phase mask technique is that a separate phase mask is require for each different Bragg wavelength. However, some wavelength tuning is possible by applying tension to the fiber during the photoimprinting process; the Bragg wavelength of the relaxed fiber will shift by $\sim$2 nm.

The phase mask technique not only yields high performance devices but is very flexible in that it can be used to fabricate gratings with controlled spectral response characteristics. For instance, the typical spectral response of a finite length grating with a uniform index modulation along the fiber length has secondary maxima on both sides of the main reflection peak. In applications like wavelength division multiplexing this type of response is not desirable. However, if the profile of the index modulation along the fiber length is given a bell-like functional shape, these secondary maxima can be suppressed [18]. The procedure is called apodization. Apodized fiber gratings have been fabricated using the phase masks technique and suppressions of the sidelobes of 30–40 dB have been achieved [19]–[21].

The phase mask technique has also been extended to the fabrication of chirped or aperiodic fiber gratings. Chirping means varying the grating period along the length of the grating in order to broaden its spectral response. Aperiodic or chirped gratings are desirable for making dispersion compensators [22]. A variety of different methods have be used to manufacture gratings that are chirped permanently or have an adjustable chirp.

Another approach to grating fabrication is the point-by-point technique [23] also developed at CRC. In this method each index perturbations of the grating are written point-by-point. For gratings with many index perturbations, the method is very not very efficient. However, it has been used to fabricate micro-Bragg gratings in optical fibers [24], but is most useful for making coarse gratings with pitches of the order of 100 μm that are required LP_{01} to LP_{11} mode converters [23] and polarization mode converters [13]. The interest in coarse period gratings has increased lately because of their use in long period fiber grating band-rejection filters [25] and fiber amplifier gain equalizers [26], [27].

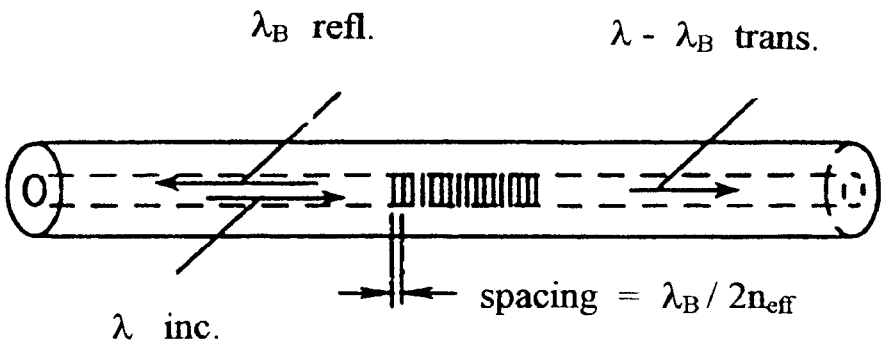

Fig. 4. Bragg resonance for reflection of the incident mode occurs at the wavelength for which the grating pitch along the fiber axis is equal to one-half of the modal wavelength within the fiber core. The back scattering from each crest in the periodic index perturbation will be in phase and the scattering intensity will accumulate as the incident wave is coupled to a backward propagating wave.

V. Fundamental Properties of Gratings

The index perturbation in the core is a periodic structure, similar to a volume hologram or a crystal lattice, that acts as a stop-band filter. A narrow band of the incident optical field within the fiber is reflected by successive, coherent scattering from the index variations. The strongest interaction or mode-coupling occurs at the Bragg wavelength λ_B given by

$$\lambda_B = 2n_{\text{eff}}\Lambda \tag{1}$$

where n_{eff} is the modal index and Λ is the grating period. Each reflection from a crest in the index perturbation is in phase with the next one at λ_B, as shown in Fig. 4, and any change in fiber properties, such as strain, temperature, or polarization which varies the modal index or grating pitch will change the Bragg wavelength. The grating is an intrinsic sensor which changes the spectrum of an incident signal by coupling energy to other fiber modes. In the simplest case, the incident wave is coupled to a counterpropagating like mode and thus reflected.

The grating filter characteristics can be understood and modeled by several approaches [28]–[32]. Coupled-mode theory is often the foundation for many of these computations. In its simplest form, this analysis leads to a single Ricatti differential equation for a modified local reflectivity $\rho(z)$, which is easily integrated by standard numerical methods. In the most general case, the index perturbation $\delta n(z)$ takes the form of a phase and amplitude-modulated periodic waveform

$$\delta n(z) = \delta n_0(z)\left[1 + m\cos\left(\frac{2\pi z}{\Lambda} + \phi\right)\right]. \tag{2}$$

Both the average refractive index and the envelope of the grating modulation, and therefore the modal index n_{eff}, usually vary along the grating length. The contrast, which is determined by the visibility of the UV fringe pattern, is given by the parameter m.

The local reflectivity $r(z)$ is the complex ratio of the forward and backward going wave amplitudes. It is related to $\rho(z)$ by a multiplicative phase factor $e^{-j\varphi}$. The modified reflectivity satisfies an equation of the form

$$\rho' = j[(4\pi/\lambda_B)(\delta n_{\text{eff}} - (\delta\lambda/\lambda_B) - \phi']\rho + j\kappa(1+\rho^2) \tag{3}$$

subject to the boundary condition $\rho(L/2) = 0$. The coupling coefficient κ is given by

$$\kappa = (\pi/\lambda)\,\delta n\, g(z)\eta \tag{4}$$

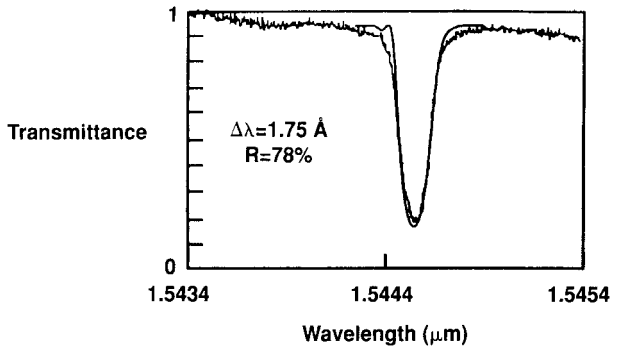

Fig. 5. Comparison of computed and measured transmission spectra for a moderate reflectivity Gaussian-apodized fiber grating. The grating length is about 10 mm as determined from measurements of the approximately Gaussian UV beam width; the grating strength ($\delta n/n = 9 \times 10^{-5}$) was inferred from the measured minimum transmittance.

where $g(z)$ is an apodization function, typically a Gaussian or raised-cosine weighting, and η is a modal overlap factor. In the case of bound-mode reflection from an unblazed grating, it is simply the fraction of modal power in the photosensitive region of the fiber index profile. If the grating has low reflectivity, then (3) can be linearized and the reflectivity spectrum $\rho(-L/2, \delta\lambda)$ will be proportional to the Fourier transform of $g(z)e^{-j\phi(z)}$. A good guide to choosing a suitable amplitude weighting for a given filter characteristic is to begin with this relationship. The reflectivity at line center ($\delta\lambda = 0$) is

$$R = \rho\rho^* = \tanh^2[(\pi/\lambda)\delta n L\overline{g}\eta] \tag{5}$$

where we neglected the chirping introduced by $\delta n_{\text{eff}}(z)$, or taken it to be a constant which offsets the line center, and adjusted the grating length by the average value $\overline{g}$ of the envelope weighting function. The reflectivity spectrum of a uniform grating can also be obtained from an analytic solution of (3) [3], [28]. It can be used to model an arbitrary grating by considering it to be a concatenated set of piecewise uniform sections and deriving a matrix transfer function for each section. The reflectivity spectrum is given by the matrix product of the set of transfer function approximations. Either modeling approach provides an accurate prediction of the reflectivity and the grating spectrum. Fig. 5 shows an example of the good agreement between the measured and computed, [in this case by integration of (3)], transmittance spectra.

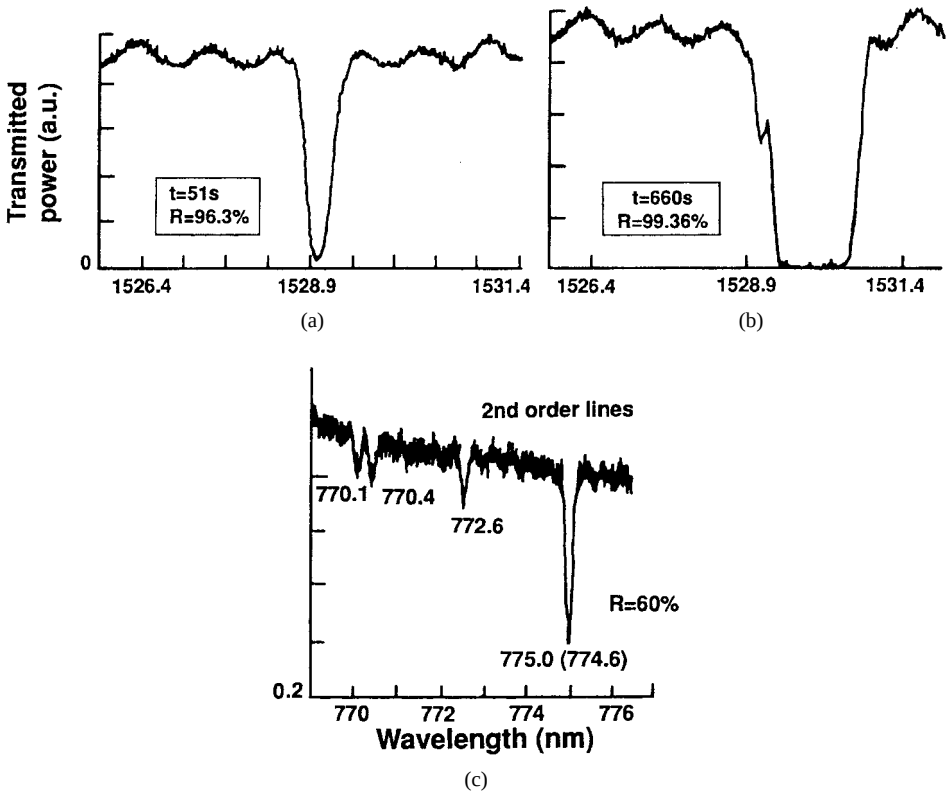

Fig. 6. A strongly reflecting grating with a large index change (a) becomes saturated and (b) after a long exposure and the spectrum broadens because the incident wave is completely reflected before reaching the end of the grating. A strongly saturated grating is no longer sinusoidal, the peak index regions are flattened and the valleys in the perturbation index distribution are sharpened. As a result, second order Bragg reflection lines (c) are observed at about one-half the fundamental Bragg wavelength and at other shorter wavelength for higher order modes. Computed second-order wavelength is shown in parenthesis.

When a grating is formed with a saturated exposure, then the effective length will be reduced as the transmitted signal is depleted by reflection. As a result, the spectrum will broaden appreciably and depart from a symmetric sinc or Gaussian-shape spectrum whose width is inversely proportional to the grating length. This is illustrated in Fig. 6(a) and (b). In addition, the cosinusoidal shape of the grating will distort into a waveform with steeper sides. A second-order Bragg line [Fig. 6(c)] will appear from the new harmonics in the Fourier spatial spectrum of the grating.

Another feature which is observed in strongly reflecting gratings with large index perturbations are small sharp spectral resonances on the short wavelength side of the grating line center. They are due to the self-chirping from $\delta n_{\text{eff}}(z)$. These features do not occur if the average index change is held constant or adjusted to be constant by a second exposure of the grating [19], [21].

A Bragg grating will also couple dissimilar modes in reflection and transmission provided two conditions are satisfied: 1) phase synchronism and 2) sufficient mode overlap in the region of the fiber that contains the grating. The phase-matching condition, which ensures a coherent exchange of energy between the modes, is given by

$$n_{\text{eff}} - \frac{\lambda}{\Lambda_z} = n_{\text{eff}} \tag{6}$$

where n_{eff} is the modal index of the incident wave and n_{eff} is the modal index of the grating-coupled reflected (a negative quantity) or transmitted wave. Note, that we have explicitly allowed for a tilt or blaze in the grating by using the grating pitch along the fiber axis Λ_z in this equation. A useful way to understand this requirement and its importance is to show the mode-coupling, phase-matching requirement graphically (Fig. 7).

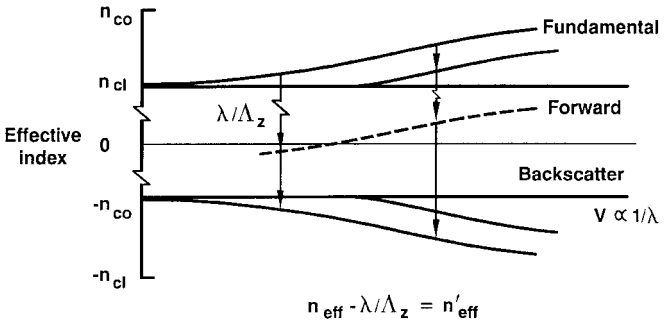

Fig. 7. Phase-matching conditions to achieve synchronous mode coupling with a fiber Bragg grating. The ratio of the wavelength λ and the grating pitch Λ_z along the fiber axis determines which type of mode (cladding or bound, backward or forward-propagating) is excited by the forward-propagating, incident LP_{01} fundamental mode.

In this illustration, we show five different types of interactions that can occur, depending on the ratio of the wavelength and pitch of the grating. Ordinary bound-mode propagation occurs when the effective index of the wave lies between the cladding and core values. A grating that reflects a like mode couples waves between the upper, forward-propagating

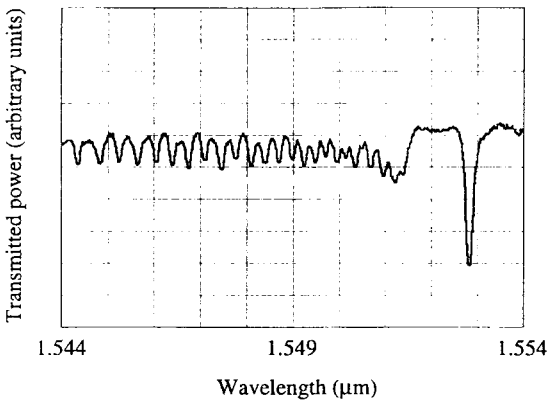

Fig. 8. Transmission spectrum of a grating in a single mode depressed-cladding fiber (AT&T Accutether) showing the fine-structure, cladding mode resonances on the short-wavelength side of the LP_{01}–LP_{01} Bragg line.

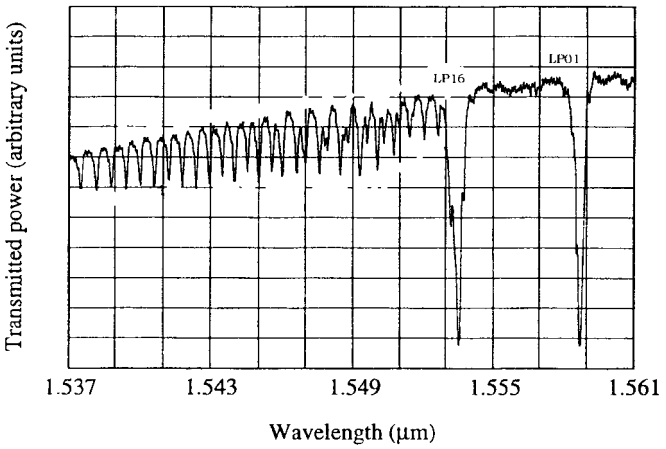

Fig. 9. Transmission spectrum of blazed grating (4.36° effective tilt angle within the core) in depressed-cladding fiber showing pronounced coupling into the asymmetric LP_{16} backward-propagating cladding mode. A tilt in the grating index profile also reduces the strength of the LP_{01}–LP_{01} reflection and produces a series of additional higher order asymmetric cladding-mode lines.

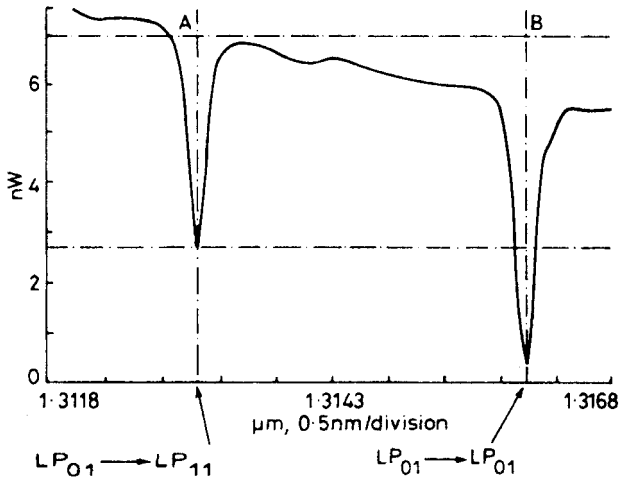

Fig. 10. Transmission spectrum of a fiber grating formed with a tilted (0.9° from normal to fiber axis) fringe pattern.

branch of the dispersion relation, to its lower negative-going, mirror image. This situation occurs when the grating has a pitch sufficiently fine that the Bragg condition (1) is obeyed. However, this same grating will also couple to other modes at shorter wavelengths; some will be reflected and or absorbed, and others will be radiated away from the fiber. The dotted line (not to scale) is a locus of wave-coupling between a forward-going fundamental mode and modes within the cladding. These interactions are seen as a series of many transmission dips in the spectrum at wavelengths that are less than the Bragg wavelength (Fig. 8) [31], [33]. No cladding modes are excited in a single mode-fiber unless the effective index of the excited mode is less than the cladding n_{cl} (with a simple matched cladding profile).

Another, quite useful situation arises if the grating period is much coarser. Now the fundamental mode *exchanges* energy in a resonant fashion with a forward-going cladding mode. The effect is similar to mode coupling in a two-core fiber or between modes in a multimoded waveguide. These gratings can be made easily with a simple transmission mask because the required pitch is a few hundred microns, as contrasted with the fine submicron pitch that is required to reflect a bound mode [25].

If the grating is tilted or radially nonuniform, then interactions will take place between symmetric and asymmetric modes (Fig. 9) [33]. For example, the grating can be used to couple the fundamental to the next lowest order mode (Fig. 10) [34], [35], as shown on the right side of Fig. 7.

VI. Applications

The characteristics of photosensitivity technology and its inherent compatibility with optical fibers has enabled the fabrication of a variety of different Bragg grating fiber devices including novel devices that were not possible previously. The FBG dispersion compensator is a good example of this latter type device. FBG's have also been incorporated in optical devices simply to act as a reflector thereby transforming the device into a practical component with enhanced performance. The semiconductor laser with a pigtail containing an FBG is an example of this type of application. Although research has concentrated on the development of Bragg grating-based fiber devices for use in fiber optic communications or fiber optic sensor systems, there are other potential applications in lidars, optical switching, optical signal processing, and optical storage. In the following, we list in table format the applications that have employed fiber Bragg gratings. Only a few of the applications are described in more detail.

Table I lists a number potential applications for fiber Bragg gratings in fiber optic communications. A particularly exciting application is the Bragg grating dispersion compensator. As a light pulse propagates down an optical fiber, it is dispersed, that is the width of the pulse broadens because the longer wavelength light lags the shorter wavelength light. Consequently, at sufficiently high data rates and/or fiber lengths, the pulses in a data stream will begin to overlap. In this way, fiber dispersion limits the maximum data that can be transmitted through a fiber. The principles underlying the operation of the FBG dispersion compensator are as follows. A dispersed light pulse with the longer wavelengths lagging the shorter wavelengths is incident on a chirped fiber grating.

TABLE I
TELECOMMUNICATION APPLICATIONS

APPLICATION	REFERENCES
Dispersion compensation	[22], [36], [37], [38], [39], [40]
Wavelength selective devices	[41]–[47]
Band-rejection filters, long-period gratings	[25]
Fiber taps	[48]
Fiber erbium amplifiers	[49]–[56]
Network monitoring and optical fiber identification	[57]–[59]
Cascaded Raman amplification at 1.3 μm	[60]
Fiber lasers	[61]–[72]
Semiconductor lasers with external Bragg grating reflector	[73]–[76]

TABLE II
OTHER APPLICATIONS

APPLICATION	REFERENCES
Optical fiber mode converters; spatial mode converters, polarization mode converters	[23], [13], [76]
Grating-based sensors	[7]
Optical single processing; delay line for phased array antennas, fiber grating compressor	[77]–[81]
Nonlinear effects in fiber Bragg gratings; optical Switching, electrooptic devices, wavelength conversion devices	[82], [83]
Optical storage; holographic storage, direct writing	[84], [85]

The longer wavelength light is reflected near the front of the grating whereas the shorter wavelength light is reflected near the back. Thus, the short wavelengths are delayed relative to the longer wavelengths. The chirped grating can be designed so that all wavelengths in the light pulse exit the reflector at the same time and the dispersion in the optical pulse in equalized. This picture is actually too simple. In reality, the relative light pulse delay as a function of wavelength is not linear but has an oscillatory behavior [36]. However, this delay characteristic can be linearized by suitably profiling or apodizing the amplitude profile of the grating [37]. In order to make a practical device, the chirped Bragg grating must be operated in the reflection mode. This can be accomplished by incorporating the chirped grating in an optical circulator or a Mach–Zehnder (MZ) interferometer. The use of chirped Bragg gratings for dispersion compensation have been demonstrated in several laboratories [38]–[41].

There are several possible applications for fiber gratings that are not related to telecommunications; some of these are listed in Table II. The most promising application FBG is in the field of optical fiber sensors. In fact, the number of fiber gratings that are used in this application may exceed that of all other applications. In the following, we describe in more detail the application of fiber gratings to sensors. We also discuss mode converters because of their potential use in FBG sensors.

VII. MODE AND POLARIZATION CONVERTERS

A resonant interaction that produces efficient bound-mode conversion within a fiber is enabled by a periodic index perturbation with a pitch that satisfies the Bragg condition for backward or forward synchronous interaction and the correct azmuthial variation to couple symmetric and asymmetric modes. A simple example is the reflection of the LP_{11} mode by a grating which is slightly tilted (Fig. 10) [34], [35]. In a fiber with a depressed index cladding, very efficient mode conversion is observed (Fig. 9) between an incident fundamental mode and a higher-order cladding mode which has a field distribution within the core that approximates an LP_{11} mode (Fig. 11) [33]. A potential application of these mode converters is introduce a larger dispersive delay into a

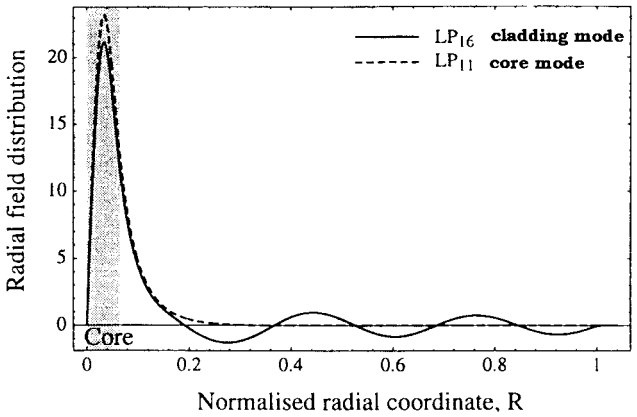

Fig. 11. Radial field distributions of the LP_{16} cladding mode and LP_{11} isolated "core" mode at the LP_{01}–LP_{16} resonance wavelength.

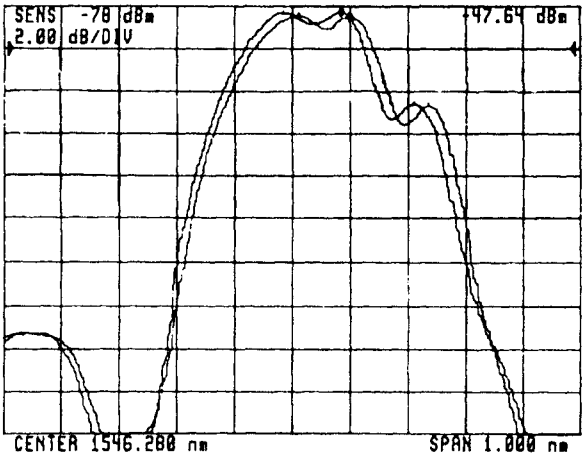

Fig. 12. Bragg wavelength shift due to UV-induced birefringence (data provided by D. R. Huber). The resonances for two orthogonal polarizations, oriented parallel and perpendicular to the polarization of the UV beam, are displaced by about 0.025 nm.

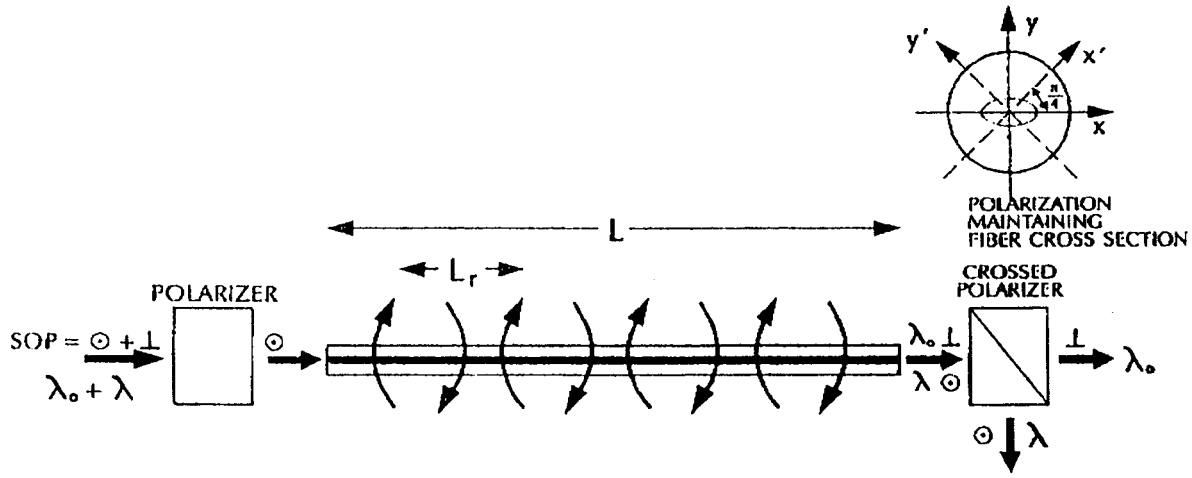

Fig. 13. Polarization rocking filter schematic showing the operating principle. If the pitch of the photo-induced birefringence L_r matches the fiber beatlength, which is wavelength dependent, then the polarization axes of the fiber will be sequentially rotated (rocked) until at length determined by the strength of the polarization coupling (UV fluenece) the modes will be rotated by 90°. A crossed polarizer can then be used to separate the resonant wavelength λ_o.

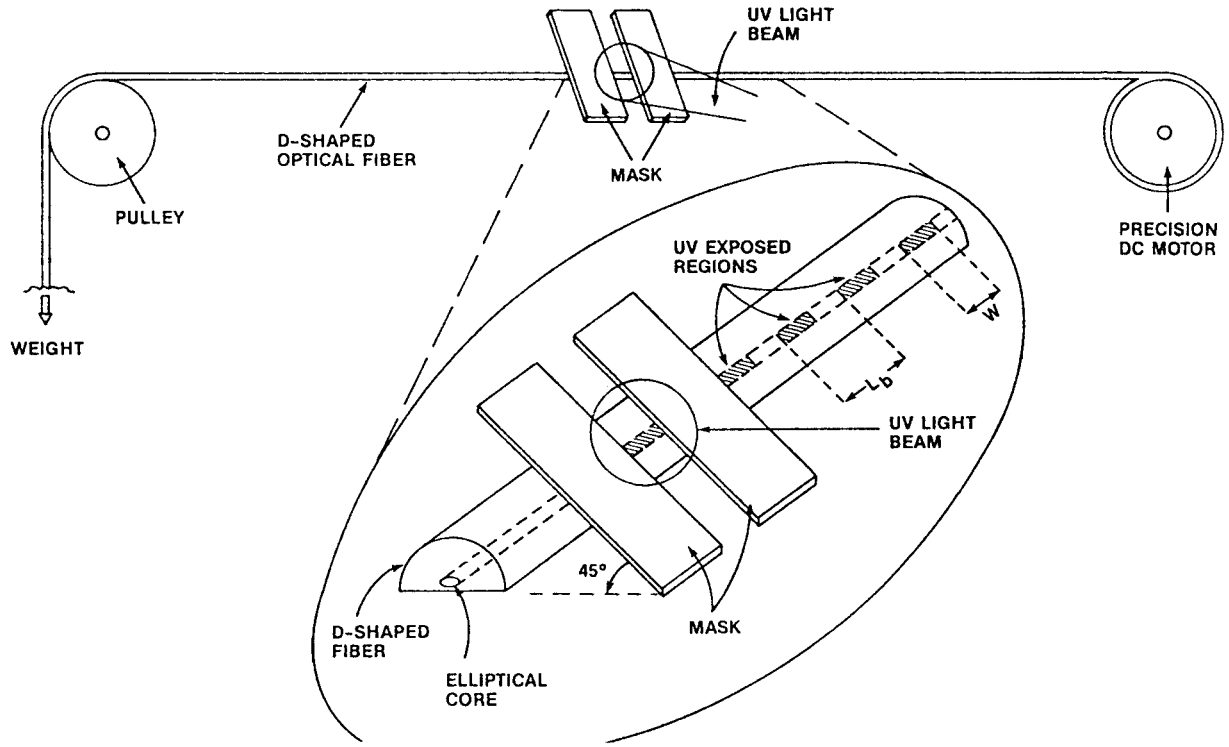

Fig. 14. Experimental arrangement for side-writing a polarization rocking filter by point-by-point exposures. A periodic, photo-induced birefringence is impressed by the polarized UV beam at an angle to the fiber polarization axes which is set by the mask orientation.

signal than would be available by just using the bound mode properties.

A fiber grating written with a UV beam that is polarized along a fiber diameter will be slightly birefringent (Fig. 12). This effect can be used to form a polarization mode converter by arranging the UV-induced, periodic birefringence (Fig. 13) to form a resonant rocking filter as shown in Fig. 14 [13], [86]. Orthogonal polarizations will be coupled in a narrow band that is controlled by the pitch and total length of the exposed segments. Resonance occurs at the wavelength for which the fiber beat length matches the rocking period or pitch of the UV-exposed regions. Low sidelobe levels and high rejection notch filtering can be achieved (Fig. 15) by the use of apodization to weight the polarization coupling coefficient along the filter length.

VIII. Grating-Based Sensors

Optical fiber sensor technology based on intra-core Bragg gratings has uses in a number of important application areas ranging from structural monitoring to chemical sensing [7], [87], [88]. Practical and cost effective systems are not far in the future judging from recent advances in grating manufacture and sensor readout instrumentation.

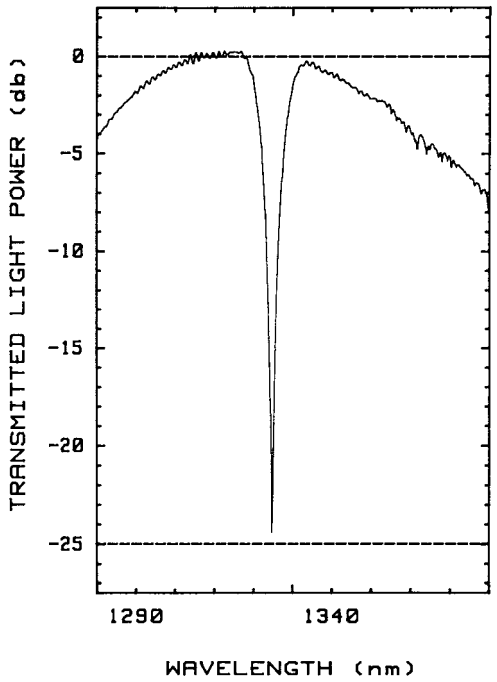

Fig. 15. High coupling-ratio rocking filter with an equivalent 99.7% transmission and 24 dB rejection. Apodization of the periodic birefringence is used to suppress the sidelobes by 7 dB.

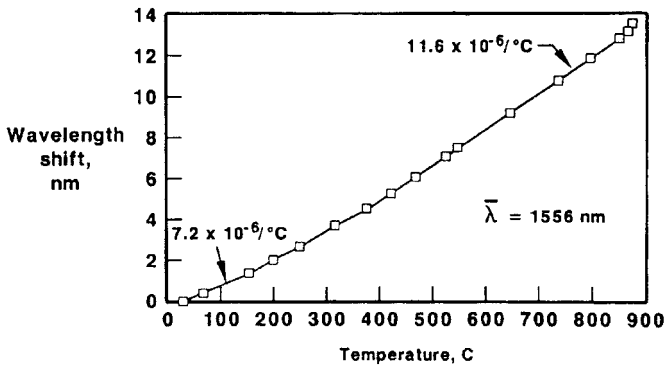

Fig. 16. Bragg grating thermal sensitivity at elevated temperature.

Any change in fiber properties, such as strain, temperature, or polarization which varies the modal index or grating pitch, will change the Bragg wavelength. The grating is an intrinsic sensor which changes the spectrum of an incident signal by coupling energy to other fiber modes. In the simplest case, the incident wave is coupled to the same counterpropagating mode and thus reflected.

A very important advantage of an FBG sensor is that it is wavelength-encoded. Shifts in the spectrum, seen as a narrowband reflection or dip in transmission, are independent of the optical intensity and uniquely associated with each grating, provided no overlap occurs in each sensor stop-band. With care in selection of the Bragg wavelengths, each tandem array of FBG sensors only registers a measurand change along its length and not from adjacent or distant transducers.

The sensitivity is governed by the fiber elastic, elastooptic and thermooptic properties and the nature of the load or strain which is applied to the structure that the fiber is attached to or

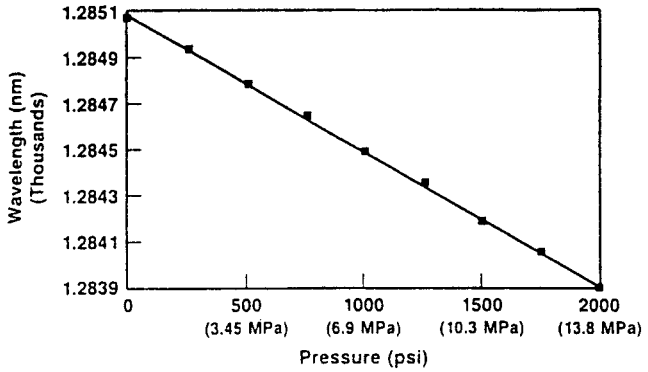

Fig. 17. Pressure sensitivity of a fiber grating coated with a thick epoxy (Hysol) jacket.

embedded within. The sensitivity to a particular measurand is no different than an other intrinsic sensor, such as a fiber interferometer. The fractional change in phase of an interferometer is the same as the fractional variation in Bragg wavelength; however, in the case of a fiber interferometer an optical leverage is realized because of the large phase path associated with a coil or long length of fiber. This multiplier in the minimum detectable measurand can be regained in the case of a FBG sensor, but not without some additional complication in the wavelength demodulation technique.

Strain shifts the Bragg wavelength through dilating or compressing the grating and changing the effective index. The amount of wavelength shift is given by

$$\frac{\delta\lambda_B}{\lambda_B} = \varepsilon_1 - (n^2/2)[p_{11}\,\varepsilon_t + p_{12}(\varepsilon_1 + \varepsilon_t)] \tag{7}$$

where the principal strains are ε_1 along the fiber axis and ε_t transverse to the fiber axis. A more complicated loading might be triaxial which would introduce a third strain component, normal to both the direction of fiber polarization and wave propagation. If the strain is homogeneous and isotropic, then (2) simplifies to its more common form

$$\begin{aligned}\frac{\delta\lambda_B}{\lambda_B} &= [1 - p_e]\varepsilon \\ &\cong 0.78\varepsilon\end{aligned} \tag{8}$$

where we have subsumed the photoelastic contributions into p_e, which is defined by

$$p_e = (n^2/2)[p_{12} - \mu(p_{11} + p_{12})]$$

in terms of the fiber Pockel's coefficients p_{ij} and μ the Poisson ratio. Typical values for the sensitivity to an applied axial strain are 1 nm/millistrain at 1300 and 0.64 nm/millistrain at 820 nm. The strain response is linear with no evidence of hysteresis at temperatures as high as 370 °C [89].

The temperature sensitivity of a bare fiber is primarily due to the thermooptic effect. It is given by

$$\begin{aligned}\frac{\delta\lambda_B}{\lambda_B} &= \alpha + \frac{1}{n}\frac{dn}{dT} \\ &\cong \frac{6.7\times 10^{-6}}{^{\circ}\mathrm{C}^{-1}}\end{aligned} \tag{9}$$

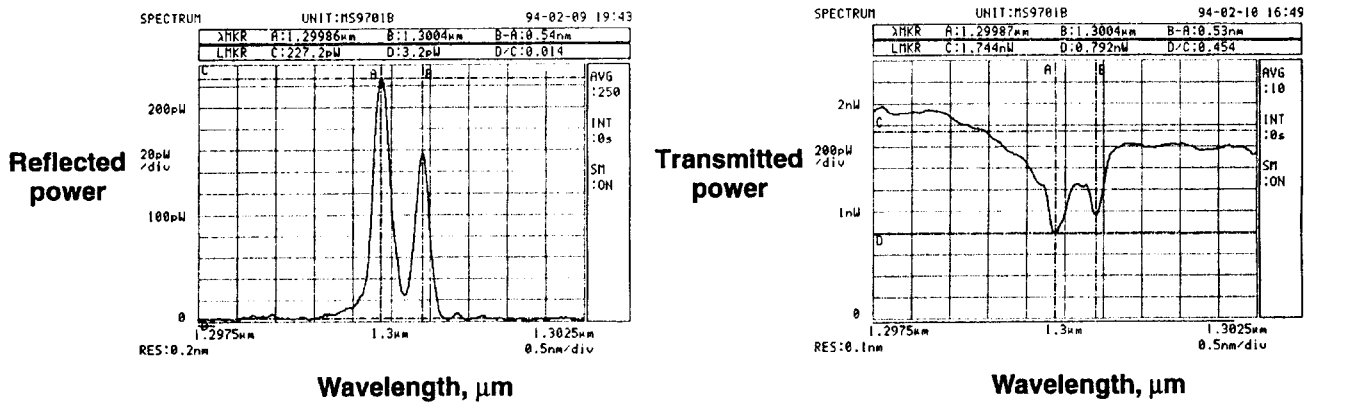

Fig. 18. Transmission and reflection spectra of a 8.3 mm long Bragg grating formed in an 18 μm-wide UV-written, buried channel waveguide. The channel and grating were formed sequentially by exposing a hydrogen loaded 6 μm germanosilicate thin film to a tightly focused beam for 25 s and then reexposing the same region to an interference pattern for 2.5 min. The grating spectrum is split into two resonances by the stressed-induced birefringence in the film.

TABLE III
APPLICATION TO PLANAR OPTICAL WAVEGUIDES

APPLICATION	REFERENCES
Planar optical waveguides	[12], [92]–[95]
Trimming of devices	[96], [97]
Optical waveguide wavelength selective devices and lasers	[98], [99]
Integration gratings onto an optoelectronic chips	[100], [101]
Direct writing of optical waveguides	[102]

up to 85 °C. A typical value for the thermal response at 1550 nm is 0.01 nm/°C. At higher temperatures, the sensitivity increases and the response becomes slightly nonlinear, as seen in Fig. 16. If the fiber is jacketed or embedded in another substance then the sensitivity can be changed and in fact nearly eliminated by the proper choice of material. This is clearly desirable if the grating is to be used as a filter or for wavelength control and stabilization of a semiconductor laser.

FBG sensor can also be used to measure pressure changes and detect acoustic signals. However, the sensitivity is far less because the glass fiber is very stiff. Some enhancement is possible by using a thick, low bulk modulus jacket, but the intrinsic response is still quite small. Large changes in pressure are detectable with simple readout systems, however complicated interferometric systems are required to use the FBG device to detect sound fields and other low-level transverse strains.

The sensitivity to pressure fields and low-frequency acoustic signals is given by a simplified form of (7)

$$\begin{aligned}\frac{\delta\lambda_B}{\lambda_B} &= \varepsilon_1 - (n^2/2)[p_{12}\varepsilon_t + p_{11}(\varepsilon_1 + \varepsilon_t)] \\ &= -2.7 \times 10^{-11}\ \text{Pa}^{-1}(\text{bare fiber}) \\ &= -10.7 \times 10^{-11}\ \text{Pa}^{-1}(\text{Hysol 109 epoxy jacket}) \quad (10)\end{aligned}$$

by recognizing that the radial and circumferential strains are equal in the core. Note that a thick jacket of low bulk-modulus material, such as Hysol, is predicted to produce a factor of 40 enhancement in the pressure response. This has been confirmed by coating a FBG sensor with a 4.8-mm diameter jacket of Hysol and placing it in a high pressure chamber [90]. The measured shift in Bragg wavelength with hydrostatic pressure is shown in Fig. 17.

The observed enhancement in sensitivity over a bare fiber is about 30.5 compared with a computed value of 39.5. The calculation assumed that the jacket was concentric and uniformly applied over the fiber which was not the case and probably contributed to a lower measured sensitivity.

An FBG sensor can also be used to measure electric and magnetic fields with special magnetostrictive and piezoelectric coatings on the fiber. These jackets produce strains within the core that cause the Bragg wavelength to shift with the magnitude of the measurand. The induced strains are small and one generally requires a readout technique which has fine resolution. Temperature variations are not a problem if RF fields are being measured, otherwise some means of temperature compensation or calibration is required.

IX. APPLICATION TO PLANAR OPTICAL WAVEGUIDES

So far, this paper has been restricted to discussing photosensitivity in optical fibers, but glass planar waveguides are also photosensitive. Consequently, there is an interest in applying photosensitivity technology to planar glass optical waveguides (see Table III). For example, the photosensitivity of thin film germanosilicate layers can be used to obtain lateral confinement by forming a buried channel waveguide with a focused UV beam. The technology can also be used to modify the modal propagation constants to trim interferometric filters and couplers and to reduce bend losses. Both waveguides and Bragg gratings can be formed with a mask or split-beam interferometer. Chemical enhancement of the photosensitivity, obtained by flame brushing, hydrogen loading or through film deposition with reduced oxygen concentrations, can be used to obtain UV-induced index changes as high as 1%.

By using the direct UV-writing technique, it is possible to form optical circuits by translating a wafer beneath a focused beam or by exposure through a mask pattern. Gratings and taps can also be formed in the channel as desired. For example, a buried channel guide and a grating were formed sequentially by exposing a sensitized commercial germanosilicate thin film to a tightly focused UV beam for 25 s and then illuminating the same region with an interference fringe pattern for an additional 2.5 m [91]. The gratings were split into a TE and TM pair with a reflectivity close to 100% as inferred from the transmission spectrum (Fig. 18) of an unpolarized broadband 1300 nm source which was butt-coupled into the guide from a standard single-mode fiber.

X. Conclusion

Fiber grating technology and its potential applications are briefly reviewed. It is shown that the technology has a broad range of applications. Currently, the most promising applications are in the fields of lightwave communications and optical fiber sensors which are based on the existence of photosensitivity in silica optical fibers and optical waveguides. However, this technology could be extended to other types of applications with the discovery of large photosensitivity in different material systems.

References

[1] K. O. Hill, Y. Fujii, D. C. Johnson, and B. S. Kawasaki, "Photosensitivity in optical fiber waveguides: Application to reflection filter fabrication," *Appl. Phys. Lett.*, vol. 32, pp. 647–649, 1978.

[2] B. S. Kawasaki, K. O. Hill, D. C. Johnson, and Y. Fujii, "Narrow-band Bragg reflectors in optical fibers," *Opt. Lett.*, vol. 3, pp. 66–68, 1978.

[3] D. K. W. Lam and B. K. Garside, "Characterization of single-mode optical fiber filters," *Appl. Opt.*, vol. 20, pp. 440–445, 1981.

[4] G. Meltz, W. W. Morey, and W. H. Glenn, "Formation of Bragg gratings in optical fibers by a transverse holographic method," *Opt. Lett.*, vol. 14, pp. 823–825, 1989.

[5] I. Bennion, J. A. R. Williams, L. Zhang, S. K., and N. J. Doran, "Tutorial Review, UV-written in-fiber Bragg gratings," *Optic. Quantum Electron.*, vol. 28, pp. 93–135, 1996.

[6] B. Poumellec, P. Niay, D. M., and J. F. Bayon, "The UV-induced refractive index grating in Ge:SiO_2 preforms: Additional CW experiments and the macroscopic origin of the change in index," *J. Phys. D, Appl. Phys.*, vol. 29, pp. 1842–1856, 1996.

[7] A. D. Kersey, "A review of recent developments in fiber optic sensor technology," *Optic. Fiber Technol.*, vol. 2, pp. 291–317, 1996.

[8] V. Garino-Canina, " Quelques propriétés optiques de l'oxyde de germanium vitreux dans l'ultraviolet, oxyde pur," *Academie des Sciences Comptes Rendus*, vol. 237, pp. 593–596, 1958.

[9] H. Hosono, Y. Abe, D. L. Kinser, Y. Abe, D. L. Kinser, R. A. Weeks, K. Muta, and H. Kawazoe, "Nature and origin of the 5-eV band in SiO_2:GeO_2 glasses," *Phys. Rev. B*, vol. 46, pp. II-445–II-451, 1995.

[10] T. Erdogan, V. Mizrahi, P. J. Lemaire, and D. Monroe, "Decay of ultraviolet-induced fiber Bragg gratings," *J. Appl. Phys.*, vol. 76, pp. 73–80, 1994.

[11] P. J. Lemaire, R. M. Atkins, V. Mizrahi, and W. A. Reed, "High pressure H_2 loading as a technique for achieving ultrahigh UV photosensitivity and thermal sensitivity in GeO_2 doped optical fibers," *Electron. Lett.*, vol. 29, pp. 1191–1193, 1993.

[12] F. Bilodeau, B. Malo, J. Albert, D. C. Johnson, K. O. Hill, Y. Hibino, M. Abe, and M. Kawachi, "Photosensitization of optical fiber and silica-on-silicon/silica waveguides," *Opt. Lett.*, vol. 18, pp. 953–955, 1993.

[13] K. O. Hill, F. Bilodeau, B. Malo, and D. C. Johnson, "Birefringent photosensitivity in monomode optical fiber: Application to the external writing of rocking filters," *Electron. Lett.*, vol. 27, pp. 1548–1550, 1991.

[14] T. E. Tasi, G. M. Williams, and E. J. Friebele, "Index structure of fiber Bragg gratings in Ge–SiO_2 fibers," *Opt. Lett.*, vol. 22, pp. 224–226, 1997.

[15] B. Poumellic, P. Guénot, I. Riant, P. Sansonetti, and P. Niay, "UV induced densification during Bragg grating inscription in Ge:SiO_2 preforms," *Opt. Mat.*, vol. 4, pp. 441–449, 1995.

[16] K. O. Hill, B. Malo, F. Bilodeau, D. C. Johnson, and J. Albert, "Bragg gratings fabricated in monomode photosensitive optical fiber by UV exposure through a phase mask," *Appl. Phys. Lett.*, vol. 62, pp. 1035–1037, 1993.

[17] D. Z. Anderson, V. Mizrahi, T. Erdogan, and A. E. White, "Production of in-fiber gratings using a diffractive optical element," *Electron. Lett.*, vol. 29, pp. 566–568, 1993.

[18] M. Matsuhara and K. O. Hill, "Optical-waveguide band-rejection filters: Design," *Appl. Opt.*, vol. 13, pp. 2886–2888, 1974.

[19] B. Malo, S. Thériault, D. C. Johnson, F. Bilodeau, J. Albert, and K. O. Hill, "Apodised in-fiber Bragg grating reflectors photoimprinted using a phase mask," *Electron. Lett.*, vol. 31, pp. 223–224, 1995.

[20] J. Albert, K. O. Hill, B. Malo, S. Thériault, F. Bilodeau, J. D. C., and L. E. Erickson, "Apodization of the spectral response of fiber Bragg gratings using a phase mask with variable diffraction efficiency," *Electron. Lett.*, vol. 31, pp. 222–223, 1995.

[21] T. A. Strasser, P. J. Chandonnet, J. DeMarco, C. E. Soccolich, J. R. Pedrazzani, D. J. DiGiovanni, M. J. Andrejco and D. S. Shenk, "UV-induced fiber grating OADM devices for efficient bandwidth utilization," in *Conf. Tech. Dig. Optic. Fiber Commun., OFC'96*, 1996, vol. 5, postdeadline paper PD8.

[22] K. O. Hill, "Aperiodic distributed-parameter waveguides for integrated optics," *Appl. Opt.*, vol. 13, pp. 1853–1856, 1974.

[23] K. O. Hill, B. Malo, K. A. Vineberg, F. Bilodeau, D. C. Johnson, and I. Skinner, "Efficient mode conversion in telecommunication fiber using externally written gratings," *Electron. Lett.*, vol. 26, pp. 1270– 1272, 1990.

[24] B. Malo, K. O. Hill, F. Bilodeau, D. C. Johnson, and J. Albert, "Point-by-point fabrication of micro-Bragg gratings in photosensitive fiber using single excimer pulse refractive index modification techniques," *Electron. Lett.*, vol. 29, pp. 1668–1669, 1993.

[25] A. M. Vengsarkar, P. J. Lemaire, J. B. Judkins, V. Bhatia, T. Erdogan, and J. E. Sipe, "Long-period fiber gratings as band-rejection filters," in *Conf. Optic. Fiber Commun., OFC'95*, San Diego, CA, 1995.

[26] E. M. Dianov, V. I. Karpov, A. S. Kukov, O. I. Medvedkov, A. M. Prokhorov, V. N. Protopopov, and S. A. Vasilév, "Gain spectrum flattening of Erbium-doped fiber amplifier using long-period grating," in *Photosensitivity and Quadratic Nonlinearity in Glass Waveguides: Fundamentals and Applications*, OSA Tech. Dig. Series, vol. 22, pp. 14–17, 1995.

[27] A. M. Vengsarkar, J. R. Pedrazzani, J. B. Judkins, P. J. Lemaire, N. S. Bergano, and C. R. Davidson, "Long-period fiber-grating-based gain equalizers," *Opt. Lett.*, vol. 21, pp. 336–338, 1996.

[28] H. Kogelnick, " Filter response of nonuniform almost-periodic gratings," *Bell Syst. Tech. J.*, vol. 55, pp. 109–126, 1976.

[29] L. A. Weller-Brophy and D. G. Hall, "Analysis of waveguide gratings: Application of Rouard's method," *J. Opt. Soc. Amer. A*, vol. 2, pp. 863–871, 1985.

[30] M. Yamada and K. Sakuda, " Analysis of almost-periodic distributed feedback slab waveguides via a fundamental matrix approach," *Appl. Opt.*, vol. 26, pp. 3474–3478, 1987.

[31] V. Mizrahi and J. E. Sipe, " Optical properties of photosensitive fiber phase gratings," *J. Lightwave Technol.*, vol. 11, pp. 1513–1517, 1993.

[32] E. Peral, J. Capmany, and J. Marti, "Iterative solution to the Gel'fand–Levitan–Mar.enko equations and application to synthesis of fiber gratings," *IEEE J. Quantum Electron.*, vol. 32, pp. 2078–2084, 1996.

[33] S. J. Hewlett, J. D. Love, G. Meltz, T. J. Bailey, and W. W. Morey, " Coupling characteristics of photo-induced Bragg gratings in depressed and matched cladding fiber," *Opt. Quantum Electron.*, vol. 28, pp. 1641–1654, 1996.

[34] W. W. Morey, G. Meltz, J. D. Love and S. J. Hewlett, "Mode-coupling characteristics of UV-written Bragg gratings in depressed-cladding fiber," *Electron. Lett.*, vol. 30, pp. 730–731, 1994.

[35] T. A. Strasser, J. R. Pedrazzani, and M. J. Andrejco, " Reflective-mode conversion UV-induced phase gratings in two-mode fiber," in *Conf. Optic. Fiber Commun., OFC'97*, 1997, OSA Tech. Dig., paper FB3, vol. 6, pp. 348–349.

[36] K. O. Hill, F. Bilodeau, B. Malo, T. Kitagawa, S. Thériault, D. C. Johnson, J. Albert, and K. Takiguchi, "Aperiodic in-fiber Bragg gratings for optical fiber dispersion compensation," in *Conf. Optic. Fiber Commun., OFC'94*, San Jose, CA, 1994.

[37] K. O. Hill, S. Thériault, B. Malo, F. Bilodeau, T. Kitagawa, D. C. Johnson, J. Albert, K. Takiguchi, T. Kataoka, and K. Hagimoto, "Chirped in-fiber Bragg grating dispersion compensators: Linearization of the

dispersion characteristic and demonstration of dispersion compensation in a 100 km, 10 Gbit/s optical fiber link," *Electron. Lett.*, vol. 30, pp. 1755–1756, 1994.
[38] J. A. R. Williams, I. Bennion, K. Sugden, and N. J. Doran, "Fiber dispersion compensation using a chirped in-fire Bragg grating," *Electron. Lett.*, vol. 30, pp. 985–987, 1994.
[39] R. Kashyap, S. V. Chernikov, P. F. McKee, and J. R. Taylor, "30 ps chromatic dispersion compensation of 400 fs pulses at 100 Gbits/s in optical fibers using an all fiber photoinduced chirped reflection grating," *Electron. Lett.*, vol. 30, pp. 1078–1080, 1994.
[40] K. O. Hill, F. Bilodeau, B. Malo, T. Kitagawa, S. Thériault, D. C. Johnson, J. Albert, and K. Takiguchi, "Chirped in-fiber Bragg grating for compensation of optical-fiber dispersion," *Opt. Lett.*, vol. 19, pp. 1314–1316, 1994.
[41] K. O. Hill, B. Malo, F. Bilodeau, S. Thériault, D. C. Johnson, and J. Albert, "Variable-spectral-response optical waveguide Bragg grating filters for optical signal processing," *Opt. Lett.*, vol. 20, pp. 1438–1440, 1995.
[42] K. O. Hill, D. C. Johnson, F. Bilodeau, and S. Faucher, "Narrow-bandwidth optical waveguide transmission filters: A new design concept and applications to optical fiber communications," *Electron. Lett.*, vol. 23, pp. 465–466, 1987.
[43] D. C. Johnson, K. O. Hill, F. Bilodeau, and S. Faucher, "New design concept for a narrowband wavelength-selective optical tap and combiner," *Electron. Lett.*, vol. 23, pp. 668–669, 1987.
[44] F. Bilodeau, K. O. Hill, B. Malo, D. C. Johnson, and J. Albert, "High-return-loss narrowband all-fiber bandpass Bragg transmission filter," *IEEE Photon. Technol. Lett.*, vol. 6, pp. 80–82, 1994.
[45] F. Bilodeau, D. C. Johnson, S. Thériault, B. Malo, J. Albert, and K. O. Hill, "An all-fiber dense-wavelength-division multiplexer/demultiplexer using photoimprinted Bragg gratings," *IEEE Photon. Technol. Lett.*, vol. 7, pp. 388–390, 1995.
[46] I. Baumann, J. Seifert, W. Nowak, and M. Sauer, "Compact all-fiber add-drop-multiplexer using fiber Bragg gratings," *IEEE Photon. Technol. Lett.*, vol. 8, pp. 1331–1333, 1996.
[47] L. Dong, P. Hua, T. A. Birks, L. Reekie, and P. S. J. Russell, "Novel add/drop filters for wavelength-division-multiplexing optical fiber systems using a Bragg grating assisted mismatched coupler," *IEEE Photon. Technol. Lett.*, vol. 8, pp. 1656–1658, 1996.
[48] G. Meltz, W. W. Morey, and W. H. Glenn, "In-fiber Bragg grating tap," in *Conf. Optic. Fiber Commun., OFC'90*, San Francisco, CA, 1990.
[49] R. Kashyap, R. Wyatt, and P. F. McKee, "Wavelength flattened saturated erbium amplifier using multiple side-tap Bragg gratings," *Electron. Lett.*, vol. 29, pp. 1025–1026, 1993.
[50] R. Kashyap, R. Wyatt, and R. J. Campbell, "Wideband gain flattened erbium fiber amplifier using a photosensitive fiber blazed grating," *Electron. Lett.*, vol. 29, pp. 154–156, 1993.
[51] J. Capmany, D. Pastor, and J. Marti', "EDFA gain equalizer employing linearly chirped apodized fiber gratings," *Microwave and Optic. Technol. Lett.*, vol. 12, pp. 158–160, 1996.
[52] C. R. Giles, T. Erdogan, and V. Mizrahi, "Simultaneous wavelength-stabilization of 980-nm pump lasers," *IEEE Photon. Technol. Lett.*, vol. 6, pp. 907–909, 1994.
[53] B. F. Ventrudo, G. A. Rogers, G. S. Lick, D. Hargreaves, and T. N. Demayo, "Wavelength and intensity stabilization of 980 nm diode lasers coupled to fiber Bragg gratings," *Electron. Lett.*, vol. 30, pp. 2147–2149, 1994.
[54] C. E. Soccolich, V. Mizrahi, T. Erdogan, P. J. LeMaire, and P. Wyscoki, "Gain enhancement in EDFA's by using fiber-grating pump reflectors," in *Conf. Optic. Fiber Commun., OFC'94*, San Jose, CA, 1994.
[55] V. L. da Silva, P. B. Hansen, L. Eskildsen, D. L. Wilson, S. G. Grubb, V. Mizrahi, W. Y. Cheung, T. Erdogan, T. A. Strasser, J. E. J. Alphonsus, S. J. R., and D. J. DiGiovanni, "15.3 dB power budget improvement by remotely pumping an EDFA with a fiber-grating pump reflector," in *Conf. Optic. Fiber Commun., OFC'95*, San Diego, CA, 1995.
[56] K. Hogari, Y. Miyajima, S. Furukawa, N. Tomita, K. Tomiyama, and M. Ohashi, "Wideband and highly reflective step-chirped fiber grating filter embedded in an optical fiber connector," *Electron. Lett.*, vol. 32, pp. 1230–1231, 1996.
[57] M. Shigehara, T. Satoh, A. Inoue, and Y. Hattori, "Optical fiber identification system using fiber Bragg gratings," in *Conf. Optic. Fiber Commun., OFC'95*, San Jose, CA, 1995.
[58] C.-K. Chan, F. Tong, L.-K. Chen, J. Song, and D. Lam, "A practical passive surveillance scheme for optically amplified passive branched optical networks," *IEEE Photon. Technol. Lett.*, vol. 9, pp. 526–528, 1997.
[59] S. G. Grubb, T. Erdogan, V. Mizrahi, T. Strasser, W. Y. Cheung, W. A. Reed, P. J. Lemaire, A. E. Miller, S. G. Kosinski, G. Nykolak, and P. C. Becker, "1.3 μm cascaded Raman amplifier in germanosilicate fibers," in *OSA Topic. Meeting, Optic. Amplifiers and Their Applications*, Breckenridge, CO, 1994.
[60] G. A. Ball, W. W. Morey, and J. P. Waters, "Nd^{3+} fiber laser utilizing intra-core Bragg reflectors," *Electron. Lett.*, vol. 26, pp. 1829–1830, 1990.
[61] G. A. Ball and W. W. Morey, "Efficient integrated Nd^{3+} fiber laser," *IEEE Photon. Technol. Lett.*, vol. 3, pp. 1077–1078, 1991.
[62] G. A. Ball and W. H. Glenn, "Design of a single-mode linear-cavity erbium fiber laser utilizing Bragg reflectors," *J. Lightwave Technol.*, vol. 10, pp. 1338–1343, 1992.
[63] G. A. Ball, W. W. Morey, and W. H. Glenn, "Standing-wave monomode erbium fiber laser," *IEEE Photon. Technol. Lett.*, vol. 3, pp. 613–615, 1991.
[64] G. A. Ball, W. H. Glenn, W. W. Morey, and P. K. Cheo, "Modeling of short, single-frequency, fiber lasers in high-gain fiber," *IEEE Photon. Technol. Lett.*, vol. 5, pp. 649–651, 1993.
[65] G. A. Ball, G. Hull-Allen, C. Holton, and W. W. Morey, "Low noise single frequency linear fiber laser," *Electron. Lett.*, vol. 29, pp. 1623–1625, 1993.
[66] M. Sejka, P. Varming, J. Hubner, and M. Kristensen, "Distributed feedback Er^{3+}-doped fiber laser," *Electronics Letters*, vol. 31, pp. 1445–1446, 1995.
[67] G. A. Ball and W. W. Morey, "Continuously tunable single-mode erbium fiber laser," *Opt. Lett.*, vol. 17, pp. 420–422, 1992.
[68] ———, "Compression-tuned single-frequency Bragg fiber laser," *Opt. Lett.*, vol. 19, pp. 1979–1981, 1994.
[69] J. D. Minelly, A. Galvanauskas, M. E. Fermann, and D. Harter, "Femtosecond pulse amplification in cladding-pumped fibers," *Opt. Lett.*, vol. 20, pp. 1797–1799, 1995.
[70] A. Galvanauskas, P. A. Krug, and D. Harter, "Nanosecond-to-picosecond pulse compression with fiber gratings in a compact fiber-based chirped-pulse-amplification system," *Opt. Lett.*, vol. 21, pp. 1049–1051, 1996.
[71] M. E. Fermann, K. Sugden, and I. Bennion, "High-power soliton fiber laser based on pulse width control with chirped fiber Bragg gratings," *Opt. Lett.*, vol. 20, pp. 172–174, 1995.
[72] D. M. Bird, J. R. Armitage, R. Kashyap, R. M. A. Fatah, and K. H. Cameron, "Narrow line semiconductor laser using fiber grating," *Electron. Lett.*, vol. 27, pp. 1115–1116, 1991.
[73] P. A. Morton, V. Mizrahi, S. G. Kosinski, L. F. Mollenauer, T. Tanbun-Ek, R. A. Logan, D. L. Coblentz, A. M. Sergent, and K. W. Wecht, "Hybrid soliton pulse source with fiber external cavity and Bragg reflector," *Electron. Lett.*, vol. 28, pp. 561–562, 1992.
[74] P. A. Morton, V. Mizrahi, P. A. Andrekson, T. Tanbun-Ek, R. A. Logan, P. Lemaire, D. L. Coblentz, A. M. Sergent, K. W. Wecht, and P. R. Sciortino, Jr., "Mode-locked hybrid soliton pulse source with extremely wide operating frequency range," *IEEE Photon. Technol. Lett.*, vol. 5, pp. 28–31, 1993.
[75] S. M. Lord, G. W. Switzer, and M. A. Krainak, "Using fiber gratings to stabilise laser diode wavelength under modulation for atmospheric lidar transmitters," *Electron. Lett.*, vol. 32, pp. 561–563, 1996.
[76] F. Bilodeau, K. O. Hill, B. Malo, D. C. Johnson, and I. M. Skinner, "Efficient, narrowband $LP_{01} \Leftrightarrow LP_{02}$ mode convertors fabricated in photosensitive fiber: Spectral response," *Electron. Lett.*, vol. 27, pp. 682–684, 1991.
[77] G. Meltz, W. W. Morey, W. H. Glenn, and J. D. Farina, "In-fiber Bragg-grating sensors," in *Proc. OFS'88*, 1988.
[78] A. Molony, C. Edge, and I. Bennion, "Fiber grating time delay element for phased array antennas," *Electron. Lett.*, vol. 31, pp. 1485–1486, 1995.
[79] H. Zmuda, R. A. Soref, P. Payson, S. Johns, and E. N. Toughlian, "Photonic beamformer for phased array antennas using a fiber grating prism," *IEEE Photon. Technol. Lett.*, vol. 9, pp. 241–243, 1997.
[80] R. A. Soref, "Fiber grating prism for true time delay beamsteering," *Fiber Integr. Opt.*, pp. 325–333, 1996.
[81] J. L. Cruz, B. Ortega, M. V. Andres, B. Gimeno, D. Pastor, J. Capmany, and L. Dong, "Chirped fiber Bragg gratings for phased-array antennas," *Electron. Lett.*, vol. 33, pp. 545–546, 1997.
[82] C. M. de Sterke, N. G. R. Broderick, B. J. Eggleton, and M. J. Steel, "Nonlinear optics in fiber gratings," *Optic. Fiber Technol.*, vol. 2, pp. 253–268, 1996.
[83] K. P. Koo and A. D. Kersey, "Optical phase amplification technique for interrogating fiber resonator sensors," in *Conf. Lasers Electro-Opt. CLEO'94*, Anaheim, CA, 1994.
[84] T. Erdogan, A. Partovi, V. Mizrahi, P. J. Lemaire, W. L. Wilson, T. A. Strasser, and A. M. Glass, "Volume gratings for holographic storage applications written in high-quality germanosilicate glass," *Appl. Opt.*,

vol. 34, pp. 6738–6743, 1995.
[85] K. O. Hill, T. Kitagawa, S. Thériault, F. Bilodeau, D. C. Johnson, B. Malo, and J. Albert, "Novel applications of photosensitivity in Ge-doped silica: Bragg grating matched filtering for optical fiber dispersion compensation and multilayer optical storage medium," in *7th Annu. Meeting, IEEE Lasers and Electro-Opt. Soc., LEOS'94*, Boston, MA, 1994.
[86] B. Malo, F. Bilodeau, D. C. Johnson, and K. O. Hill, " Rocking filters written in photosensitive birefringent fiber: Suppression of sidelobes in filter wavelength response," in *Conf. Optic. Fiber Commun., OFC'92*, 1992, OSA Tech. Dig. vol. 5, postdeadline paper PD23, pp. 404–407.
[87] G. Meltz, " Overview of fiber grating-based sensors," in *Proc. SPIE, Distributed and Muliplexed Sensors VI*, 1996, vol. SPIE-2838, pp. 2–23.
[88] A. D. Kersey, M. A. Davis, T. A. Berkoff, D. G. Bellemore, K. P. Koo, and R. T. Jones, "Progress toward the development of practical fiber Bragg grating instrumentation systems," in *Proc. SPIE, Fiber Optic and Laser Sensors XIV*, 1996, vol. SPIE-2839, pp. 40–64.
[89] W. W. Morey, G. Meltz, and J. M. Weiss, " Recent advances in fiber grating sensors for utility industry applications," in *Proc. SPIE, Self Calibrated Intelligent Optical Sensors and Systems*, 1995, vol. SPIE-2594, pp. 90–98.
[90] ———, "Evaluation of a fiber Bragg grating hydrostatic pressure sensor," in *Proc. 8th Optic. Fiber Sensor Conf.*, 1992, postdeadline paper PD4.
[91] G. Meltz and W. W. Morey, "Photoinduced refractivity in germanosilicate waveguides," in *Proc. Integr. Photon. Res. Conf.*, 1994, postdeadline paper PD6, pp. PD6-1–PD6-4.
[92] T. Kitagawa, K. O. Hill, D. C. Johnson, B. Malo, J. Albert, S. Thériault, F. Bilodeau, K. Hattori, and Y. Hibino, "Photosensitivity in P_2O_5–SiO_2 waveguides and its application to Bragg reflectors in single-frequency Er^{3+}-doped planar waveguide laser," in *Proc. Optic. Fiber Commun. Conf., OFC'94*, San Jose, CA, 1994.
[93] T. A. Strasser, T. Erdogan, A. E. White, V. Mizrahi, and P. J. Lemaire, "Ultraviolet laser fabrication of strong, nearly polarization-independent Bragg reflectors in germanium-doped silica waveguides on silica substrates," *Appl. Phys. Lett.*, vol. 65, pp. 3308–3310, 1994.
[94] G. D. Maxwell, B. J. Ainslie, D. L. Williams, and R. Kashyap, "UV written 13 dB reflection filters in hydrogenated low loss planar silica waveguides," *Electron. Lett.*, vol. 29, pp. 425–426, 1993.
[95] D. Bosc, B. Loisel, M. Moisan, N. Devoldere, F. Legall, and A. Rolland, "Temperature and polarization insensitive Bragg gratings realized on silica waveguide on silicon," *Electron. Lett.*, vol. 33, pp. 134–136, 1997.
[96] R. Kashyap, G. D. Maxwell, and B. J. Ainslie, "Laser-trimmed four-port bandpass filter fabricated in single-mode photosensitive Ge-doped planar waveguide," *IEEE Photon. Technol. Lett.*, vol. 5, pp. 191–194, 1993.
[97] M. Svalgaard, C. V. Poulsen, A. Bjarklev, and O. Poulsen, "Direct UV writing of buried singlemode channel waveguides in Ge-doped silica films," *Electron. Lett.*, vol. 30, pp. 1401–1403, 1994.
[98] T. Kitagawa, F. Bilodeau, B. Malo, S. Thériault, J. Albert, D. C. Johnson, K. O. Hill, K. Hattori, and Y. Hibino, "Single-frequency Er^{3+}-doped silica-based planar waveguide laser with integrated photo-imprinted Bragg reflectors," *Electronics Letters*, vol. 30, pp. 1311–1312, 1994.
[99] G. E. Kohnke, T. Erdogan, T. A. Strasser, A. E. White, M. A. Milbrodt, C. H. Henry, and E. J. Laskowski, "Planar waveguide Mach–Zender bandpass filter fabricated with single exposure UV-induced gratings," in *OFC'96, Optic. Fiber Commun.*, San Jose, CA, 1996.
[100] T. Tanaka, H. Takahashi, M. Oguma, T. Hashimoto, Y. Hibino, Y. Yamada, Y. Itaya, J. Albert, and K. O. Hill, "External cavity laser composed of laser diode and UV written grating integrated on Si," *Electron. Lett.*, vol. 32, pp. 1202–1203, 1996.
[101] G. D. Maxwell, R. Kashyap, G. Sherlock, J. V. Collins, and B. J. Ainslie, "Demonstration of a semiconductor external cavity laser using a UV written grating in a planar silica waveguide," *Electron. Lett.*, vol. 30, pp. 1486– 1487, 1994.
[102] G. D. Maxwell and B. J. Ainslie, "Demonstration of a directly written directional coupler using UV-induced photosensitivity in a planar silica waveguide," *Electron. Lett.*, vol. 31, pp. 95–96, 1995.

Kenneth O. Hill for a photograph and biography, see this issue, p. 1262.

Gerald Meltz (M'87), photograph and biography not available at the time of publication.